Anomalous behaviour of thermodynamic properties at successive phase transitions in $(NH_4)_3GeF_7$

Evgeniy V. Bogdanov[a,b,*], Andrey V. Kartashev[a,c], Evgeniy I. Pogoreltsev[a,d], Mikhail V. Gorev[a,d], Natalia M. Laptash[a,e], Igor N. Flerov[a,d]

[a]*Kirensky Institute of Physics, Federal Research Center KSC SB RAS, 660036 Krasnoyarsk, Russia*

[b] *Institute of Engineering Systems and Energy, Krasnoyarsk State Agrarian University, 660049 Krasnoyarsk, Russia*

[c]*Astafijev Krasnoyarsk State Pedagogical University, 660049 Krasnoyarsk, Russia*

[d] *Institute of Engineering Physics and Radioelectronics, Siberian Federal University, 660074 Krasnoyarsk, Russia*

[e]*Institute of Chemistry, Far Eastern Department of RAS, 690022 Vladivostok, Russia*

*Corresponding author.
Present address: Kirensky Institute of Physics
Akademgorodok 50, bld. 38,
Krasnoyarsk, 660036, Russia
Tel.: +7-(391)-249-45-07;
Fax: +7-(391)- 2430-89-23
Email address: evbogdanov@iph.krasn.ru

Abstract:

Heat capacity, thermal dilatation, susceptibility to hydrostatic pressure and dielectric properties associated with succession of three phase transitions below room temperature in double fluoride salt $(NH_4)_3GeF_7$ were studied. A possible transformation into the parent *Pm-3m* cubic phase was not observed up to the decomposition of compound. Nonferroelectric nature of structural distortions was confirmed. The DTA under pressure studies revealed a high temperature stability of two phases: *P4/mbm* and *Pbam*. The entropies of the phase transitions agree well with the model of structural distortions. Analysis of the thermal properties associated with the individual phase transitions in the framework of thermodynamic equations has shown a high reliability of the data obtained.

Keywords Phase transition; Fluorides; Heat capacity; Entropy; Thermal expansion; High pressure

1. Introduction

In accordance with [1-8], a lot of complex fluoride compounds demonstrate a very interesting peculiarity associated with an ability to change significantly the symmetry of crystal lattice under chemical pressure variation as the result of the cationic substitution. From the perspective of material science, this point is rather important because it allows one to obtain the necessary characteristics of crystals using the relationship between chemical composition, structure and physical properties. The series of the double fluoride salts $(NH_4)_3MeF_7 = (NH_4)_2MeF_6 \cdot NH_4F = (NH_4)_3[MeF_6]F$, which are known for many years, is a very good example exhibiting the different room temperature symmetries of the crystal lattice depending on the size of the central metal atom Me [9-14]. Moreover, recently it was shown that their symmetry as well as physical properties can be also changed by temperature and/or external hydrostatic pressure variations, which lead to the structural phase transitions [15-21].

It was found that the decrease of the Me atom size from Sn to Ti and then to Ge is accompanied by increasing number of the structural transformations as well as changing their temperatures. Upon heating, $(NH_4)_3SnF_7$ undergoes at $T_0 = 356$ K a reversible transition between the two cubic phases Pa-$3 \leftrightarrow Pm$-$3m$ [18]. Two intermediate tetragonal phases exist between the cubic phases in $(NH_4)_3TiF_7$ Pa-3 $(T_2 = 292$ K$) \leftrightarrow P4/mbm$ $(T_1 = 358$ K$) \leftrightarrow 4/m$ (sp. gr. is not yet determined) $(T_0 = 430$ K$) \leftrightarrow Pm$-$3m$ [15, 16], however, the phase Pm-$3m$ is observed only under pressure [17]. Moreover, the pressure increase leads also to the successive disappearance of both tetragonal phases in titanium double fluoride salt at the two triple points and as a result the direct transformation Pa-$3 \leftrightarrow Pm$-$3m$ takes place at $p > 0.41$ GPa. Calorimetric experiments have shown that an entropy change in $(NH_4)_3SnF_7$, $\Delta S_0 = 32.5 \pm 2.5$ J/mol·K, is very close to the sum of the entropy changes in $(NH_4)_3TiF_7$, $\Sigma \Delta S_i = \Delta S_0 + \Delta S_1 + \Delta S_2 = 33.5 \pm 3.5$ J/mol·K, connected with the three structural transformations [17, 19]. Such a large value of the entropic parameters could be considered as associated with ordering-disordering of some structural elements in both heptafluorides. Indeed, octahedra $[SnF_6]$ and tetrahedra $[NH_4]$ were found disordered in the Pm-$3m$ phase and totally ordered in Pa-3 phase at least for $(NH_4)_3SnF_7$ [18]. However, the phase transition Pa-$3 \leftrightarrow P4/mbm$ in titanium compound was characterized as reconstructive transformation because both space groups are not connected by the group-subgroup relationship [15, 16]. X-ray studies have proved this statement: structural distortions at this transition were found connected, on the one hand, with the ordering of $[NH_4]$ and $[SnF_6]$ polyhedra and, on the other, with a significant rotation of the octahedra ordered already in $P4/mbm$ phase, large displacements of some F atoms and formation of hydrogen bonds [16]. The contribution of the entropy change associated with the phase transition Pa-$3 \leftrightarrow P4/mbm$ to the total entropy change in $(NH_4)_3TiF_7$ is rather large $\Delta S_2 = 22.7 \pm 1.6$ J/mol K, that is, 68 % from $\Sigma \Delta S_i$ [17].

According to the X-ray and polarizing-optic studies, $(NH_4)_3GeF_7$ exhibits below room temperature a sequence of transformations $P4/mbm$ $(T_1 = 279.4$ K$) \leftrightarrow Pbam$ $(T_2 = 270$ K$) \leftrightarrow P2_1/c$ $(T_3 = 227$ K$) \leftrightarrow Pa$-3 [21]. Phase transition into the

cubic phase *Pm*-3*m* was not found at least up to 380 K. A mechanism of the phase transitions was also found associated with the appearance and shortening of hydrogen bonds as the result of the fluorine atom displacement from the center of the octahedron [FN$_6$] leading to its distortion. Upon cooling, two nonequivalent octahedra, Ge1F$_6$ and Ge2F$_6$, were suggested being successively rotated around one and two axes at first and second transformations, respectively. The phase transition into the cubic phase *Pa*-3 was postulated as reconstructive.

In the present paper, we continue investigation of the effect of the central atom size on the thermodynamic properties of the double fluoride salts (NH$_4$)$_3$*Me*F$_7$ undergoing different successions of the structural phase transitions. A detailed study of the heat capacity, thermal dilatation, dielectric properties and sensitivity to hydrostatic pressure of (NH$_4$)$_3$GeF$_7$ was performed over wide range of temperature. The data obtained on entropy, permittivity and $T - p$ phase diagram are discussed in connection with mechanism and nature of the structural distortions.

2. Experimental Results

A double fluoride salt (NH$_4$)$_3$GeF$_7$ was prepared by fluorination of GeO$_2$ of a reagent grade using ammonium hydrogen difluoride, NH$_4$HF$_2$. The synthesis was performed at $150 - 200$ °C while the beginning of the reaction was detected even at room temperature under grinding the mixture of the initial components. Numerous experiments have shown that in order to be succeeded preparing a pure compound, it is necessary to take at least the double excess of NH$_4$HF$_2$ relative to stoichiometric reaction: GeO$_2$ + 3.5·NH$_4$HF$_2$ = (NH$_4$)$_3$GeF$_7$ + 0.5·NH$_3$ + 2·H$_2$O. The cake obtained in this way was water-leached. Slow evaporation of the final solution under ambient conditions led to the formation of colorless prismatic single crystals of (NH$_4$)$_3$GeF$_7$.

Measurements using differential scanning microcalorimrter (DSM) and differential thermal analysis (DTA) under high pressure were performed on the powdered samples of (NH$_4$)$_3$GeF$_7$. The samples for heat capacity with adiabatic calorimeter, thermal dilatation and dielectric measurements were prepared as quasi-ceramic disk-shaped pellets of $4 - 8$ mm diameter and 1.0 - 4.0 mm thickness under pressure without heat treatments because of the presence of ammonium ions.

The compound synthesized was characterized in two steps. First, X-ray analysis was carried out, which revealed that at room temperature, (NH$_4$)$_3$GeF$_7$ has a tetragonal symmetry (sp. gr. *P*4/*mbm*, Z = 2), consistent with the data of [21]. No additional phases were observed in the sample. Second, in order to evaluate temperature and entropy of the phase transitions observed in [21], preliminary calorimetric investigations of the crystal (NH$_4$)$_3$GeF$_7$ grown were performed on several samples with the mass about 0.2 g using DSM. Samples were put in an aluminium sample holder and examined in a He gaseous atmosphere in a wide temperature range $100 - 450$ K. Heat capacity, $C_p(T)$, measurements were performed upon heating and cooling at a rate of $dT/d\tau = 16$ K/min and 8 K/min.

No reversible heat capacity anomalies were observed above room

temperature. Consequently, at ambient pressure, the tetragonal phase $P4/mbm$ of $(NH_4)_3GeF_7$ was stable up to the beginning of decomposition, which was detected at ~ 430 K. Below room temperature, three reproducible anomalies of $C_p(T)$ were found in heating mode at temperatures $T_1 = 279 \pm 1$ K, $T_2 = 269 \pm 1$ K and $T_3 = 228 \pm 1$ K, which agree well with temperatures of the structural transformations found in the optical studies with the polarizing microscope [21]. Fig. 1 depicts the temperature dependence of the excess heat capacity, ΔC_p, associated with the successive phase transitions and determined as the difference between the total molar heat capacity C_p and non-anomalous lattice contribution C_{latt}.

At a rate of temperature cycling equal to 16 K/min, all the phase transition temperatures demonstrate hysteresis: $\delta T_1 \approx 3$ K, $\delta T_2 \approx 3$ K, $\delta T_3 \approx 11.5$ K. The decrease of $dT/d\tau$ down to 8 K/min is accompanied by strong decrease of $\delta T_1 \approx 1.5$ K and $\delta T_2 \approx 1.5$ K and small decrease in the value of $\delta T \approx 10.5$ K. This fact as well as the shape of the ΔC_p peaks allowed one to conclude that $(NH_4)_3GeF_7$ undergoes phase transitions of the second order at T_1 and T_2, and first order at T_3.

A closeness of the T_1 and T_2 temperatures prevents to determine the enthalpy changes separately for each phase transitions $P4/mbm \leftrightarrow Pbam$ and $Pbam \leftrightarrow P2_1/c$. The total enthalpy associated with both transformations $\Sigma\Delta H_{1+2} = 2400 \pm 170$ J·mol^{-1} was determined by integration of the $\Delta C_p(T)$ function. The enthalpy for transformation at T_3 is one and a half times greater: $\Delta H_3 = 3600 \pm 260$ J·mol^{-1}.

A push-rod dilatometer (NETZSCH model DIL-402C) with a fused silica sample holder was used to study the thermal expansion. Measurements were performed in a dry He flux in the temperature range 120 – 380 K with a heating rate of 3 K·min^{-1}. The results were calibrated, by taking quartz as the standard reference, to remove the influence of system thermal expansion. The uncertainty in dilatation measurements was about 5 %.

The results of the thermal dilatation study are shown in Fig. 2. The temperature behaviour of the volume deformation, $\Delta V/V_0 = 3 \cdot (\Delta L/L_0)$, and the coefficient of thermal volume expansion, β, demonstrates anomalous peculiarities in the temperature region where $(NH_4)_3GeF_7$ undergoes successive phase transitions. There are two kinks at T_1 and T_2 and a strong jump at T_3 and three peaks in the $\Delta V/V_0(T)$ and $\beta(T)$ curves, respectively (Fig. 2 a, b). The $\beta(T)$ dependence above T_1 was chosen as the lattice contribution β_{lat} and extrapolated into low temperature phases. Fig. 2 b and c show that anomalous contribution $\Delta\beta = \beta - \beta_{lat}$ in the coefficient of the thermal dilatation is positive and negative at $P4/mbm$ (T_1) $\leftrightarrow Pbam$ and $Pbam$ (T_2) $\leftrightarrow P2_1/c$ (T_3) $\leftrightarrow Pa$-3 phase transitions, respectively. The temperatures of the lows and highs on the $\beta(T)$ dependence were chosen as the phase transition temperatures T_i. The reconstructive transformation $P2_1/c$ (T_3) $\leftrightarrow Pa$-3 is accompanied by a very strong negative volume deformation change, $\delta(\Delta V/V_0) \approx -1.05 \cdot 10^{-2}$.

In order to see that the ferroelastic phase transitions $P4/mbm \leftrightarrow Pbam \leftrightarrow P2_1/c$ in $(NH_4)_3GeF_7$ [21] are not accompanied by appearance of the ferroelectricity, the behaviour of dielectric properties was also examined. The

measurements of permittivity and dielectric losses were performed by means of an E7-20 immitance meter at a frequency of 1 kHz upon heating/cooling at a rate of about 0.7 K/min in the temperature range 100 – 300 K. Electrodes on quasi-ceramic disk-shaped pellets were formed by conducting glue covered the opposite flat sides of the sample.

The temperature dependence of the permittivity ε shows the pronounced step-wise anomaly about 2 units only at T_3 which is accompanied by large thermal hysteresis $\delta T_3 \approx 14$ K observed also on the $tg\delta(T)$ dependence (Fig. 3). Such a behaviour is associated with a large volume strain of the crystal lattice mentioned above at the reconstructive transformation $P2_1/c \leftrightarrow Pa\text{-}3$. A strong increase of $\varepsilon(T)$ and $tg\delta(T)$ above 250 K is, most likely, associated with the dielectric losses in the quasi-ceramic sample prepared without heat treatment. The results obtained confirm the absence of the ferroelectric properties and, thus, prove the data of structural analysis where the centrosymmetric phases $Pbam$ and $P2_1/c$ were chosen below T_1 and T_2, respectively [21].

The effect of hydrostatic pressure on the temperatures of the heat capacity anomalies associated with the phase transitions was experimentally studied by DTA. A powdered sample with a mass of ~ 0.02 g was placed in a small copper container glued onto one of two junctions of a germanium-copper thermocouple. A quartz sample cemented to the other junction was used as a reference substance. The system, mounted in such a manner, was placed inside the piston-cylinder type vessel associated with the pressure multiplier. Pressure of up to 0.5 GPa was generated using silicon oil as the pressure-transmitting medium. Pressure and temperature were measured with a manganin gauge and copper-constantan thermocouple with accuracies of about $\pm\ 10^{-3}$ GPa and $\pm\ 0.3$ K, respectively.

The $T-p$ phase diagram was built from the results of measurements for increasing pressure and temperature cycles (Fig. 4). It seen that $T_3 \approx 253$ K exceeds significantly the T_3 values observed in other experiments above which is due, most likely, to the highest rate of the temperature change in DTA-measurements and a strong first order of the phase transition $P2_1/c \leftrightarrow Pa\text{-}3$ accompanied by very large hysteresis. Fig. 4 also demonstrates that all the phase boundaries with a high degree of reliability are linear. Positive value of the baric coefficient $dT_1/dp = 10$ K/GPa is characteristic only for the phase transition $P4/mbm \leftrightarrow Pbam$ which means a slow narrowing of the temperature range of the $P4/mbm$ phase existence with pressure increase. Due to a difference between the values of $dT_2/dp = -47$ K/GPa and $dT_3/dp = -34$ K/GPa, the phase $P2_1/c$ disappears at the triple point with rather low pressure $p_{trp} \approx 0.3$ GPa and $T_{trp} \approx 245$ K. Thus, the orthorhombic phase $Pbam$ is the most stable under pressure. Indeed, at pressure above p_{trp}, the $Pbam \leftrightarrow Pa\text{-}3$ transformation is characterized by the largest rate of the temperature decrease under pressure, $- 86$ K/GPa.

In order to get a possibility to discuss the mechanism of the structural distortions in $(NH_4)_3GeF_7$, a precise determination of the excess heat capacity and integral thermodynamic characteristics associated with the phase transitions was carried out via measurements using a homemade adiabatic calorimeter with two thermal shields [22]. Over the whole temperature range investigated, the

inaccuracy in the heat capacity determination did not exceed (0.2 -0.4) %. The mass of the sample was 0.1253 g. Calorimetric measurements were carried out using continuous ($dT/dt \approx 0.15$ K/min) and discrete ($\Delta T \approx 2.5$ -3.0 K) modes of heating. In the vicinity of the first order transformation at T_3, investigations were also carried out using a method of quasistatic thermograms with an average heating of $dT/dt \approx 10^{-2}$ K/min. The heat capacity of the heater and contact grease was measured in a separate experiment.

Fig. 5a shows the temperature dependence of the molar heat capacity $C_p(T)$ of $(NH_4)_3GeF_7$. In accordance with a succession of the phase transitions $P4/mbm \leftrightarrow Pbam \leftrightarrow P2_1/c \leftrightarrow Pa$-3 found in optic and X-ray investigations [21], three $C_p(T)$ anomalies were observed with maximum values at $T_1 = 277.4 \pm 0.1$ K, $T_2 = 267.8 \pm 0.1$ K и $T_3 = 229.1 \pm 0.05$ K.

The $T(t)$ dependence obtained in the heating mode demonstrates that the large latent heat $\delta H_3 \approx 3100 \pm 150$ J/mol is smeared within the narrow temperature interval $T_3 \pm 1.2$ K. Due to very large value of the temperature hysteresis $\delta T_3 > 10$ K observed in the birefringence, DSM and permittivity measurements, it was not possible to measure the δH_3 value upon cooling with an adiabatic calorimeter.

In order to determine the enthalpy and entropy of the phase transitions, separation of the total heat capacity C_p on a regular lattice C_L and anomalous ΔC_p contributions was performed. For this purpose, the experimental data taken far from the transition points ($T < 187$ K and $T > 294$ K) were fitted using a linear combination of Debye and Einstein terms $C_L = K_D C_D + K_E C_E$, where

$$C_D(T) = 9R \left(\frac{T}{\Theta_D}\right)^3 \int_0^{\frac{\Theta_D}{T}} \frac{x^4 \exp(x)}{(\exp(x)-1)^2} \, dx, \tag{1}$$

$$C_E(T) = 3R \left(\frac{\Theta_E}{T}\right)^2 \frac{\exp(\Theta_E/T)}{(\exp(\Theta_E/T)-1)^2}, \tag{2}$$

and K_D, K_E, Θ_D, Θ_E are fitting parameters. The characteristic Debye's and Einstein's temperatures were estimated as follows: $\Theta_D = 224$ K and $\Theta_E = 557$ K. A dashed line in Fig. 5a presents the lattice contribution $C_L(T)$. The average deviation of the experimental data from the smoothed curve does not exceed ~ 0.5%. It seen that anomalous contributions ΔC_p associated with the individual phase transitions exist in a wide range of the temperature and are overlapped. Therefore, on the first stage, we were able to determine only the total enthalpy and entropy changes by integration over the entire range of existence of ΔC_p: $\Sigma \Delta H_i = \int \Delta C_p dt = 6100 \pm 400$ J/mol and $\Sigma \Delta S_i = \int (\Delta C_p/T) dT = 25.5 \pm 1.8$ J/mol·K. Fig. 6c demonstrates the behaviour of the entropy associated with all the phase transitions in $(NH_4)_3GeF_7$.

3. Discussion

The phases $P4/mbm$, $Pbam$ and $P2_1/c$ are connected with each other by the group-subgroup relationship [21] and the phase transitions between them are of the

second order. In such a case, the Landau thermodynamic theory can be used to analyze the physical properties of $(NH_4)_3GeF_7$ in the two intermediate phases. In accordance with one of the consequences of this theory [23], the value of $(\Delta C_p/T)^{-2}$ is a linear function of the temperature below a point of the second order transformation:

$$\left(\frac{\Delta C_p}{T}\right)^{-2} = \frac{2B}{A_T^2} + \frac{12C}{A_T^3}(T_0 - T). \qquad (3)$$

Here T_0 is a temperature of phase transition, A_T, B and C are the coefficients of the thermodynamic potential $\Delta\Phi(p,T,\eta) = A_T(T - T_0)\cdot\eta^2 + B\cdot\eta^4 + C\cdot\eta^6$, where η is order parameter.

Fig. 6a shows that the temperature behaviour of the $(\Delta C_p/T)^{-2}$ values associated with the phase transitions at T_1 and T_2 follows linear dependences with different slope and over different ranges of the temperature $T_1 - T \approx 3$ K and $T_2 - T \approx 18$ K. Information on the elastic susceptibility of $(NH_4)_3GeF_7$ associated with the A_T coefficient is absent. Therefore using (3), we can only determine the relationship between the coefficients of the thermodynamic potential to characterize the proximity (N) of the second-order phase transitions to the tricritical points T_{k1} and T_{k2} (Fig. 6a). Here, T_{ki} is a temperature where $(\Delta C_p/T)^{-2} = 0$. For the second order transformations, parameter N presents the combination of the coefficients of the thermodynamic potential above: $N = (B^2/3A_T CT_0)^{0.5} = [(T_k - T_0)/T_0]^{0.5}$ [23]. Small values of the parameters $N_{T1} = 0.11$ and $N_{T2} = 0.08$ show that both phase transitions, $P4/mbm \leftrightarrow Pbam$ and $Pbam \leftrightarrow P2_1/c$, are rather close to the tricritical point.

Group-theory analysis has shown [21] that the phase transitions of the second order in $(NH_4)_3GeF_7$ are associated with the emergence of instability at the same $(1/2, 1/2, 0)$ k_{18}–point (M) of the Brillouin zone of $P4/mbm$ and driven by the $M_1^- \oplus M_4^-$ and M_5^- irreducible representations, respectively, characterized by the different order parameters. Thus, the contribution of $\Delta C_p(T)$ existed in the phase $Pbam$ can be extrapolated into $P2_1/c$ as it is shown in Fig. 6b. The same procedure was used to restore the $\Delta C_p(T)$ function below T_2 and T_3. In such a case the anomalous behaviour of $\Delta C_p(T)$ near the phase transition into the cubic phase Pa-3 appears as shown in Fig. 6c. Then, we were able to determine the magnitudes of the individual entropy changes for each phase transition: $\Delta S_1 = 7.5 \pm 0.5$ J/mol·K; $\Delta S_2 = 4.5 \pm 0.3$ J/mol·K and $\Delta S_3 = 13.5 \pm 1.0$ J/mol·K.

To ensure the validity of the approach used to determine the heat capacities associated with the individual phase transitions, we compared the results of three independent experiments: $\beta(T)$, $C_p(T)$ and $T(p)$. Using the data on $\Delta\beta$ and ΔC_p at T_1 and T_2 in the framework of the Ehrenfest equation, the values of relative baric coefficients were determined $dT_1/dp = 13$ K/GPa and $dT_2/dp = -43$ K/GPa, which are in a good agreement with the results of direct measurements above. The value $dT_3/dp = -39$ K/GPa calculated using the Clausius-Clapeyron equation also agrees well with the baric coefficient determined in DTA experiments with pressure.

By the way, it should be noted that the reconstructive transformation $P2_1/c \leftrightarrow Pa$-3 is accompanied by a very strong volume deformation change,

$\delta(\Delta V/V_0) \approx -1 \%$. which is close to $\delta(\Delta V/V_0) \approx -0.9 \%$ observed at phase transition Pa-$3 \leftrightarrow Pm$-$3m$ in $(NH_4)_3SnF_7$ [19]. From our point of view, it means that in spite on different successions of the phase transitions the main contribution into the strain of the crystal lattice is associated with a reconstruction of structure during the formation of the Pa-3 phase.

The results obtained show that chemical pressure change associated with the substitution of the central atom Me effects significantly on the stability of both cubic phases, Pm-$3m$ and Pa-3. The decrease of the unit cell volume in $(NH_4)_3TiF_7$ compared to $(NH_4)_3SnF_7$ is accompanied by the strong increase in the temperature of the phase transition into the Pm-$3m$ phase: 356 K (Sn) and 430 K (Ti). In such a case one can assume that in germanium compound with smaller ionic radius of the central atom, the Pm-$3m$ phase can be realized at higher temperature compared to $(NH_4)_3TiF_7$. A stability of the Pa-3 phase is also strongly affected by the chemical pressure. However, decrease in a size of the central atom is accompanied by decrease in temperature of the transformation into this phase. Moreover, this temperature decreases also with increase in pressure in compounds with $Me = $ Ti, Ge.

The Pm-$3m$ phase is a parent phase for fluoride double salts which was observed in $(NH_4)_3TiF_7$ and $(NH_4)_3SnF_7$ at high and ambient pressure, respectively [17, 18]. Successive transformations in titanate compound and the direct phase transition in stannate compound between the cubic phases Pm-$3m$ and Pa-3 are accompanied by close values of the entropy change, respectively $\Sigma\Delta S_i = 33.5$ J/mol·K [17] and $\Delta S = 32.5$ J/mol·K [19]. In $(NH_4)_3GeF_7$, the cubic phase Pm-$3m$ was not found neither in X-ray and optic studies [21] nor in the present investigations. Entropic parameter for germanium compound, $\Sigma\Delta S_i = 25.5 \pm 1.8$ J/mol·K, is very close to that associated with the direct transformation $P4/mnc \leftrightarrow Pa$-$3$ in $(NH_4)_3TiF_7$: $\Delta S_2 = 22.7 \pm 1.6$ J/mol·K [17]. However, it is worth to remind that despite the tetragonal symmetry at room temperature, both fluorides are characterized by different models of structural disorder [17, 21]. One third of the [TiF_6] octahedra and, very likely, [NH_4] tetrahedra are disordered in $(NH_4)_3TiF_7$, while in $(NH_4)_3GeF_7$ only tetrahedral NH_4 groups are disordered. The common feature of both fluorides is the total ordering of all the structural elements in the cubic phase Pa-3. Thus, the closeness of entropic parameters in titanium and germanium double salts is most likely coincidence.

According to [21], a tilting of the ordered GeF_6 octahedra at T_1 and T_2 is very large (> 20°) and, thus, it can contribute significantly into related entropies. In such a case, the individual entropy changes, $\Delta S_1 = 0.90 \cdot R$ and $\Delta S_2 = 0.54 \cdot R$, in $(NH_4)_3GeF_7$ can be considered as "intermediate" between the values characteristic for order-disorder and displacive mechanisms of structural distortions.

4. Conclusions

Experimental study of heat capacity, thermal dilatation, susceptibility to hydrostatic pressure and dielectric properties revealed some similarities and

peculiarities in the behaviour of double fluoride salt $(NH_4)_3GeF_7$ compared to previous studied $(NH_4)_3TiF_7$ [17] and $(NH_4)_3SnF_7$ [19].

All the properties studied show anomalous behaviour associated with the succession of the three phase transitions $P4/mbm$ ($T_1 = 277.4$ K) $\leftrightarrow$ $Pbam$ ($T_2 = 267.8$ K) $\leftrightarrow$ $P2_1/c$ ($T_3 = 229.1$ K) $\leftrightarrow$ Pa-3 found in $(NH_4)_3GeF_7$ [21]. Upon heating, a transformation into the parent Pm-3m cubic phase was not observed up to the temperature of decomposition (~ 430 K).

The behaviour of dielectric properties proves the nonferroelectric nature of transformations.

An increase in hydrostatic pressure leads, first, to disappearance of the monoclinic $P2_1/c$ phase at the triple point with $p_{trp} = 0.3$ GPa and, second, to broadening of the orthorhombic $Pbam$ phase. At $p > p_{trp}$, the temperature range of the cubic Pa-3 phase existence is quickly narrowed. The reliability of the results obtained is proved by good agreement between values of the baric coefficients measured experimentally and calculated using thermodynamic equations.

Rather close temperatures of the phase transitions prevented to obtain information on the thermodynamic properties associated with the individual transformations. Despite the different symmetry of the tetragonal room temperature phase in $(NH_4)_3GeF_7$ and $(NH_4)_3TiF_7$ (sp. gr. $P4/mnc$), the total entropy changes were found to be almost equal. Analysis of the heat capacity in the two intermediate phases of germanium compound using the Landau thermodynamic theory allowed one to determine contributions of each phase transition into the excess heat capacity and entropy. Not very large entropy changes at T_1 and T_2, $\Delta S_1 = 7.5$ J/mol·K; $\Delta S_2 = 4.5$ J/mol·K, agree with a model of structural distortions [21] where elements of displacive and order-disorder mechanisms were assumed. Reconstructive transformation into Pa-3 phase associated with complex structural distortions including a formation of the hydrogen bonds is accompanied by very large values of the entropy, $\Delta S_3 = 13.5$ J/mol·K, and volume strain, $\delta(\Delta V/V_0) \approx -1$ %, changes.

Acknowledgements

References

[1] J.S. Thrasher, S.H. Strauss, Inorganic Fluorine Chemistry: Toward the 21st Century. ACS Symposium Series 555, American Chemical Society, Washington, DC, (1994).
[2] T. Nakajima, B. Zemva, A. Tressaud, Advanced Inorganic Fluorides, Elsevier, Amsterdam, (2000).
[3] T. Nakajima, H. Groult, Fluorinated Materials for Energy Storage, Elsevier, Amsterdam, (2005).

[4] A. Tressaud, Functionalized Inorganic Fluorides, Wiley-Blackwell, Chichester. (2010).

[5] M. Leblanc, V. Maisonneuve, A. Tressaud, Crystal chemistry and selected physical properties of inorganic fluorides and oxide–fluorides, Chem.Rev.115 (2015) 1191–1254.

[6] I. Flerov, M.Gorev, K.Aleksandrov, A.Tressaud, J.Grannec, M.Couzi, Phase transitions in elpasolites (ordered perovskites), Mater. Sci. Eng. R - Rep.24 (1998) 81–151.

[7] J. Ravez, Ferroelectricity in solid state chemistry, C. R. Acad. Sci. Paris. Ser. IIc, Chim./Chem. 3 (2000) 267–283.

[8] J.F. Scott, R. Blinc, Multiferroic magnetoelectric fluorides: why are there so many magnetic ferroelectrics? J. Phys. :Condens.Matter 23 (113202) (2011) 17 pp.

[9] D.L. Deadmore, W.F. Bradley, Acta Crystallogr. 15 (1962) 186–189.

[10] J.L. Hoard, M.B. Williams, J. Am. Soc. 64 (1942) 633–637.

[11] C. Plitzko, G. Meyer, Z. Kristallogr, NCS 213 (1998) 475.

[12] C. Plitzko, G. Meyer, Z. Anorg, Allg. Chem. 623 (1997) 1347–1348.

[13] U. Reusch, E. Schweda, Mater. Sci. Forum 378–381 (2001) 326–330.

[14] A. Vasiliev, N. Laptash, Inst. of Physics Krasnoyarsk, Russia, ICDD Grant-in-Aid, 2003.

[15] S. V. Mel'nikova, E. I. Pogoreltsev, I. N. Flerov, N. M. Laptash, J. Fluorine Chem., 165, (2014) 14–19.

[16] M. S. Molokeev, S. V. Misjul, I. N. Flerov, N. M. Laptash, Acta Crystallogr., Sect. B: Struct. Sci., 70 (2014) 924–931.

[17] E. I. Pogoreltsev, I. N. Flerov, A. V. Kartashev, E. V. Bogdanov, N. M. Laptash, J. Fluorine Chem., 168 (2014) 247–250.

[18] I. N. Flerov, M. S. Molokeev, N. M. Laptash, A. A. Udovenko, E. I. Pogoreltsev, S. V. Mel'nikova, S. V. Misyul, J. Fluorine Chem., 178 (2015) 86–92.

[19] A.V.Kartashev, M.V.Gorev, E.V.Bogdanov, I.N.Flerov, N.M.Laptash, J. Solid State Chem., 237 (2016) 269-273.

[20] E. I. Pogoreltsev, E. V. Bogdanov, A. V. Kartashev, M. S. Molokeev, I. N. Flerov N. M. Laptash, Ferroelectrics, 501 (2016) 20–25.

[21] S. V. Mel'nikova, M. S. Molokeev, N. M. Laptashc, S. V. Misyul, Dalton Trans., 45 (2016) 5321–5327.

[22] A. V. Kartashev, I. N. Flerov, N. V. Volkov, K. A. Sablina, Phys. Solid State, 50 (2008) 2115–2120.

[23] Aleksandrov, K. S.; Flerov, I. N. The applications of the thermodynamic theory to structural phase transitions close to the tricritical point. Fiz. Tverd. Tela. 21 (1979) 327−336.
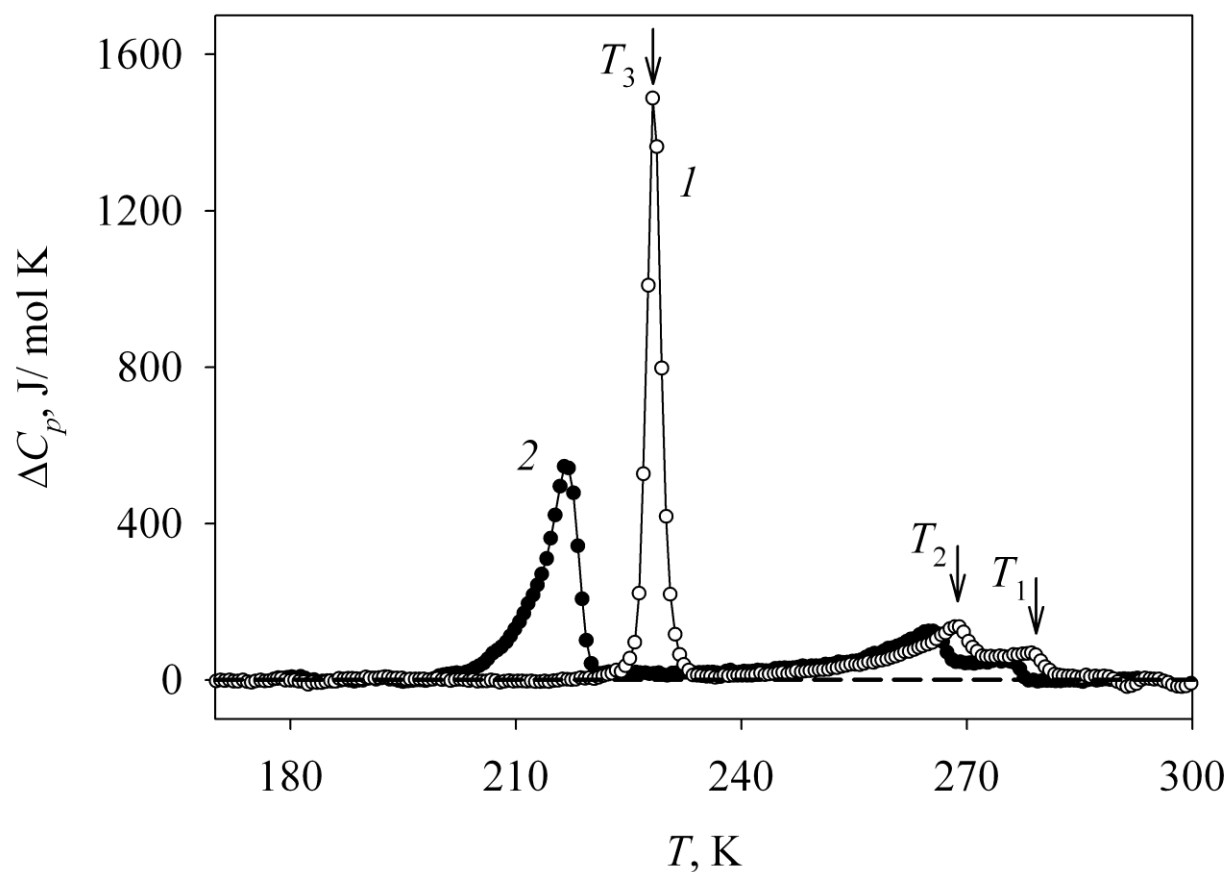
Fig. 1. Temperature dependence of ΔCp upon heating (*1*) and cooling (*2*) obtained in DSM experiments at the rate ~ 16 K/min for one of the $(NH_4)_3GeF_7$ samples.
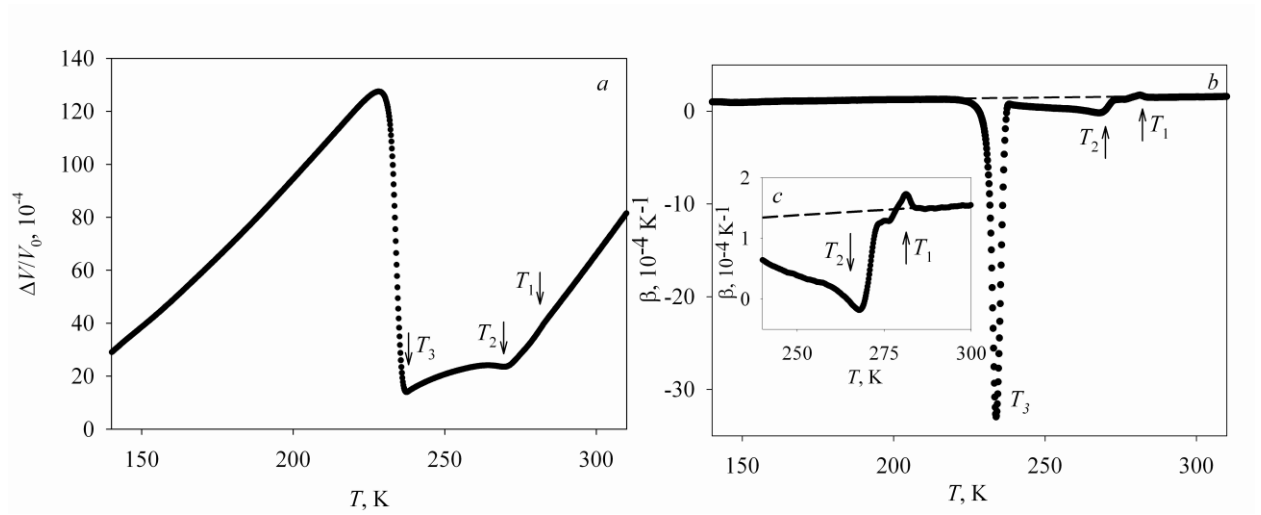
Fig. 2. Temperature dependence of (*a*) strain $\Delta V/V_0$ and (*b*) the volume thermal expansion coefficient β of $(NH_4)_3GeF_7$. (*c*) Anomalous behaviour of β at T_1 and T_2. Dashed line is a lattice contribution β_{lat}.
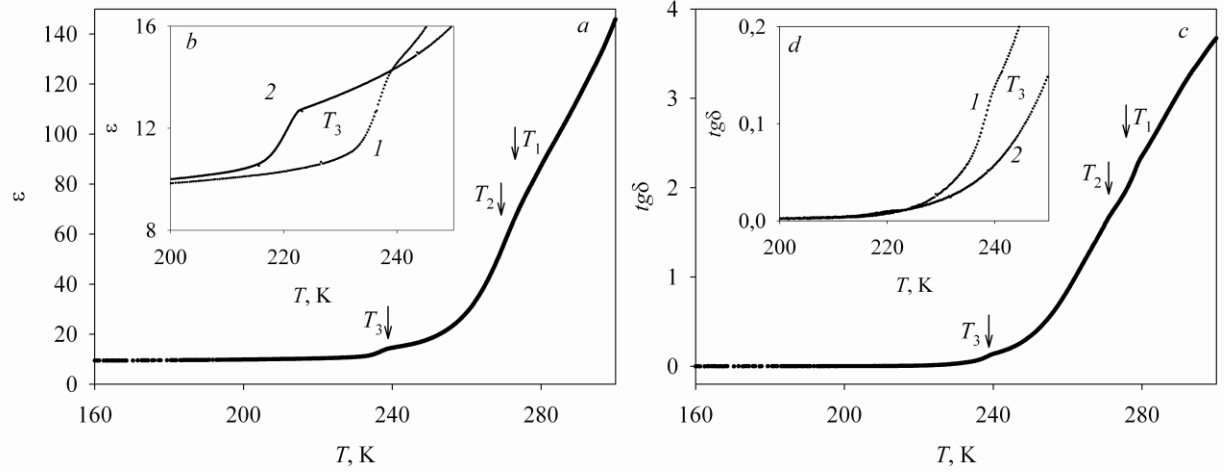
Fig. 3. Temperature dependencies of (a, b) the permittivity ε and (c, d) the dielectric loss tangent $tg\delta$ over a wide temperature range and near T_3 upon heating (*1*) and cooling (*2*).
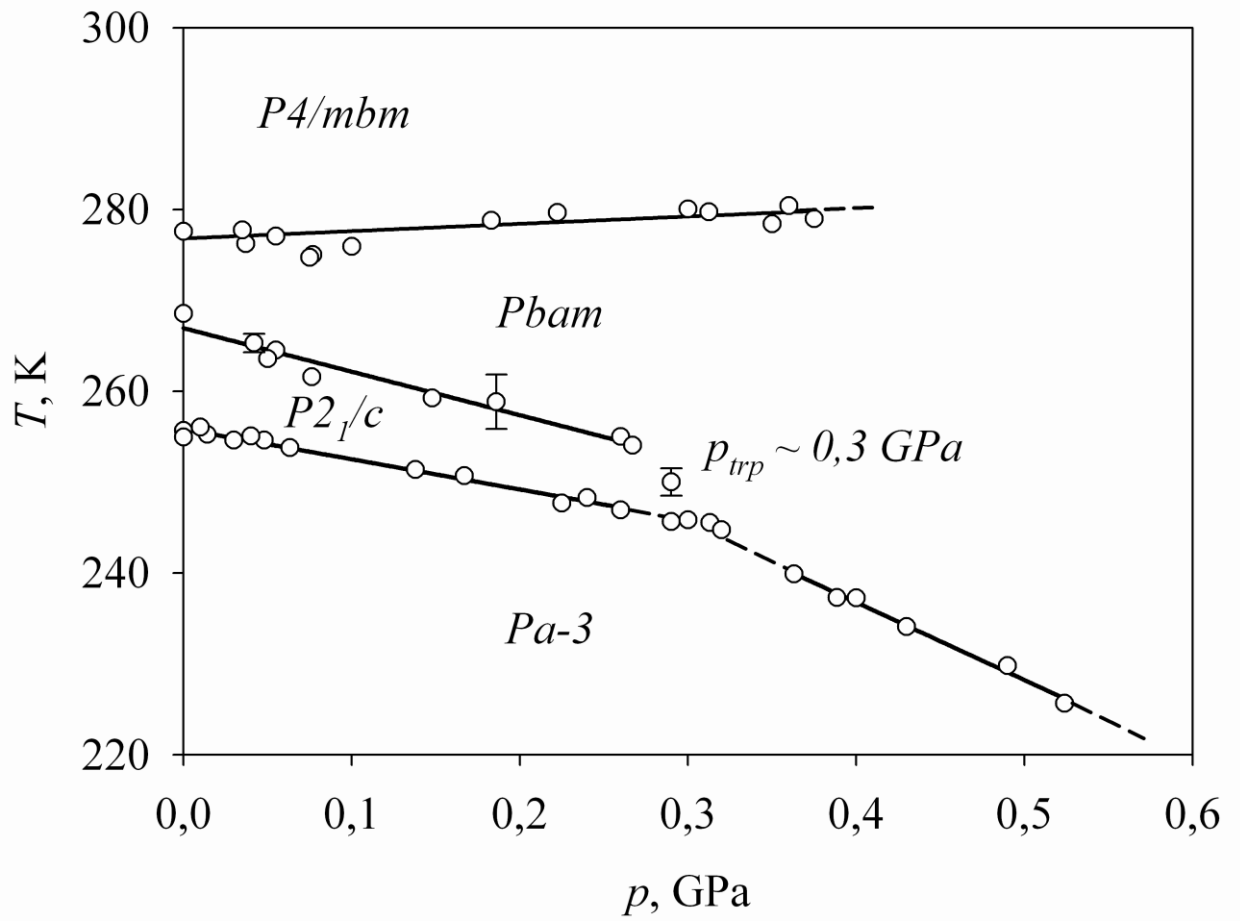
Fig. 4. The temperature–pressure phase diagram of a crystal of $(NH_4)_3GeF_7$.
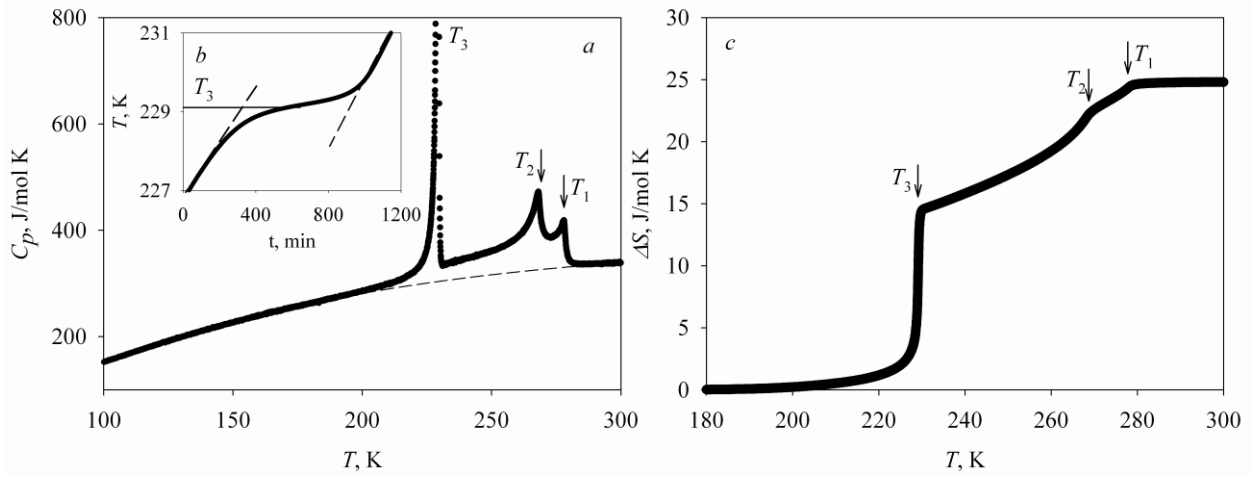
Fig. 5. (*a*) Temperature dependence of the molar heat capacity in a wide temperature range. Dashed line: lattice heat capacity. (*b*) Thermogram in the heating mode in the vicinity of T_3. (*c*) Temperature dependence of the total excess entropy change.
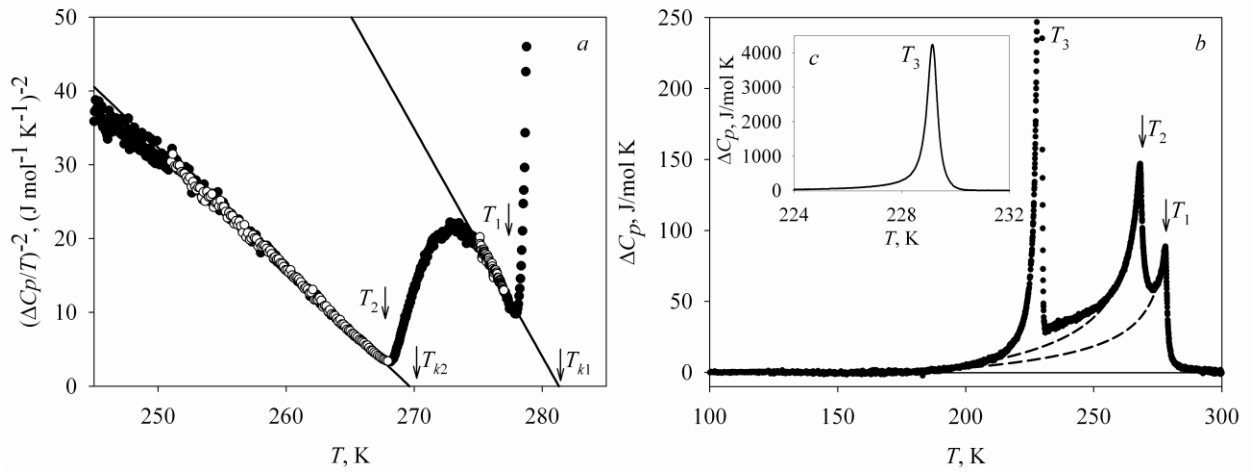
Fig. 6. (*a*) Temperature dependence of the square of the inverse excess heat capacity. (*b*) Temperature dependence of the total excess heat capacity. Dashed lines present the behaviour of contributions into $\Delta C_p(T)$ in the intermediate (*Pbam* and *P2$_1$/c*) and low temperature *Pa*-3 phases (*c*) Temperature dependence of excess heat capacity around T_3.